Neuroradiology: Imaging characteristics of an unusual, high-grade angiocentric glioma: A case report and review of the literature.

Aguilar et al.

Imaging characteristics of an unusual, high-grade angiocentric glioma:
A case report and review of the literature.

Hector N. Aguilar[1], Ryan W. Hung[1], Vivek Mehta[2], Trevor Kotylak[1*]

1. Department of Radiology & Diagnostic Imaging, Faculty of Medicine and Dentistry, University of Alberta, Edmonton, Alberta, Canada

2. Division of Neurosurgery, Department of Surgery, Faculty of Medicine and Dentistry, University of Alberta, Edmonton, Alberta, Canada

* **Correspondence:** Trevor Kotylak, MD, 2A2.41 Walter C Mackenzie Health Sciences Centre, Department of Radiology & Diagnostic Imaging, Faculty of Medicine and Dentistry, University of Alberta, Edmonton, AB, Canada T6G 2R7
(✉ tkotylak@ualberta.ca)

ABSTRACT

Angiocentric gliomas have recently been reclassified as a separate central nervous system tumor. Few cases have been reported, and most of those correspond to slow-growing, low-grade neoplasms in very young pediatric patients. Here we describe magnetic resonance imaging findings (including diffusion imaging, spectroscopy and tractography) in an unusual higher-grade neoplasm with pathologic features suggestive of an angiocentric glioma in a 15-year-old male. The tumor had mild heterogeneous enhancement on magnetic resonance imaging, and a low apparent diffusion coefficient (9.9×10^{-4} mm^{2}s^{-1}), consistent with an intermediate-to-high cellularity tumor. Spectroscopic imaging showed elevated choline/phosphocreatine and choline/N-acetyl aspartate ratios, suggesting an unusually aggressive tumor. We conclude that angiocentric glioma should not be excluded from consideration at primary diagnosis, particularly in teenaged patients nearing adulthood.

CASE REPORT

CASE REPORT

A 15-year-old male of South Asian descent presented to the emergency department with a four-month history of progressively worsening weakness and numbness of the left side of his body, beginning with his left hand and arm, and followed by involvement of his left leg. He also complained of left-sided facial weakness, drooling, blurred vision, and intermittent headaches with photophobia. Further review of systems, previous medical history, and family history were non-contributory. Physical examination revealed several neurological findings: bilateral papilledema, sluggish pupil responses to light, a left-sided facial droop, reduced strength in the left upper and lower extremities, and a right-sided cranial nerve VI palsy. Routine laboratory investigations were normal.

Diagnostic imaging workup began with unenhanced computed tomography (CT) of the head (Fig. 1a, Siemens SOMATOM Definition AS+, 64-slice multidetector CT, sequential axial, 4.8 mm slice thickness), which showed a heterogeneous, intraaxial ovoid mass centered on the right frontal lobe, measuring 6.7 cm in maximal diameter. The lesion produced both local mass effect with subfalcine herniation and effacement of the anterior horn of the lateral ventricle, as well as global mass effect with approximately 6 mm of right-to-left midline shift. No hemorrhage or calcification of the lesion was demonstrated, and there was no significant white matter edema. The initial differential diagnosis for this right frontal lobe mass had included a dysembryoplastic neuroepithelial tumor, ganglioglioma or gangliocytoma. Urgent neurosurgical consult and magnetic resonance (MR) imaging were advised.

Neuroradiology: Imaging characteristics of an unusual, high-grade angiocentric glioma: A case report and review of the literature.

Aguilar et al.

MR imaging of the brain and whole spine were subsequently performed (Siemens MAGNETOM Avanto 1.5T), with sequences including sagittal and axial T1-weighted (T1, with echo time (TE) of 12 msec, TR 283 msec, 5 mm slice thickness), 3D gradient echo T1 (MP-RAGE, TE 3.4 msec, TR 1900 msec), axial T2-weighted (T2, TE 105 msec, TR 5662 msec, 5 mm slice thickness), axial diffusion-weighted, (DWI, TE 121 msec, TR 5200 msec, 5 mm slice thickness, with b factors of 0, 500 and 1000) and axial diffusion tensor tractography (DTT, TE 88 msec, TR 3236 msec, 5 mm slice thickness) imaging. MR spectroscopy was performed by selecting a 2.0 x 2.0 x 2.0 cm cube within a solid portion of the tumor anteromedially, and performing short (TE 30 msec), medium (TE 135 msec) and long (TE 270 msec) spectral acquisitions in this tissue volume. This was followed by gadolinium administration (Gadovist, 0.2 ml/kg intravenously), then sagittal T1 (TE 12 msec, TR 382 msec) and a 3D gradient echo T1 sequence (MP-RAGE, TE 3.9 msec, TR 2130 msec).

MR imaging confirmed an ovoid T1 heterogeneously hypointense, T2 heterogeneously hyperintense intraaxial mass in the right anterior frontal lobe extending from the periventricular region up to the vertex (Fig. 1b, c and d). Irregular areas of T1 hyperintensity within the central and inferior portions of the mass were interpreted to be in keeping with hemorrhage. Several small T2 hyperintense cavitary regions were also present within the mass. The mass was associated with adjacent T2 hyperintensity, diffusely involving the white matter of the frontoparietal regions bilaterally. There was again compression of the anterior horn of the right lateral ventricle, causing leftward shifting of midline by approximately 1.2 cm. The lateral, 3rd and 4th ventricles were not affected. Post-gadolinium, the mass demonstrated mild, heterogeneous, internal enhancement with numerous pial feeder vessels, but without other enhancing lesions (compare Fig. 1e and d).

Several additional imaging studies were obtained, as shown in Fig. 2. On DTT (Fig. 2 a), the mass caused displacement and splaying of the craniocaudally-oriented white matter fibers of the right corona radiata and centrum semiovale. Superiorly, the posterior margin of the mass is approximately 1.5-2.0 cm anterior to the precentral gyrus. However, inferiorly, the posteromedial aspect of the mass abutted and splayed the fibers radiating into the anterior limb and genu of the internal capsule. On DWI (Fig. 2 b and c), the mass was predominantly similar to brain tissue in its apparent diffusion coefficient (ADC). Anteromedially, in a solid, partially enhancing portion of the mass, corresponding to the region from which spectroscopic data were obtained, the ADC measured 9.9×10^{-4} mm^2s^{-1}. On MR spectroscopy (Fig. 2 d), the choline/phosphocreatine ratio was 5.3, 7.0, and 5.3 at TE of 30, 135 and 270 msec, respectively. The choline/N-acetyl aspartate (NAA) ratio was 2.8, 12.6, and 11.9 at TE of 30, 135, and 270 msec. A lactate/lipid doublet was observed to flip at a TE of 135 msec, suggesting the presence of lactate within the lesion. The spinal cord signal was unremarkable, with no enhancing masses seen (Fig. 3).

The patient underwent gross total resection of the tumor (post-surgical MR, Fig. 3), with specimens sent for pathology. The histological findings from a biopsy smear and frozen sections corresponded to a malignant glioma with anaplastic features. The neoplasm exhibited an infiltrating growth pattern with abundant entrapped neurofilament protein-immunoreactive axons, and diffuse immunoreactivity for glial fibrillary acidic protein (GFAP). Perivascular formations were present, both linearly along the long axes and radially as classic perivascular pseudorosettes, thought neither feature was numerous. Cellular elongation was also present. These features raised the possibility of angiocentric glioma although one classic feature, subpial palisading, was absent. EMA staining revealed impression dot-like staining for microlumens, which supported ependymal differentiation. Further, numerous mitoses, vascular proliferation and focal necroses were present. In sum, the lesion might be a high-grade variant of angiocentric glioma (AG), of uncertain WHO grade (III versus IV), given the rarity of such findings.

Postoperatively the patient's hemiparesis improved but he was left with profoundly diminished visual acuity (20/400 in both eyes). The patient received fractionated radiation therapy (59.4 Gy). In addition, postoperatively the patient developed a seizure disorder that was well controlled on medical management with Tegretol (Carbamazepine). On post-surgical imaging performed on post-operative day number 1, and also four weeks after the surgery, the tumor bed exhibited features indistinguishable from post-surgical inflammation.

Post-surgery, the patient experienced some lower leg paresthesias and difficulty initiating urination, which resolved spontaneously. He denied any seizure activity. Unfortunately, approximately six months post-surgery he began to develop worsening left hemiparesis. These findings coincided with a thickened and nodular appearance of the tumor bed (Fig. 4). The patient then required a repeat right frontal craniotomy for resection. The histopathological features of this resection were consistent with a clinically recurrent/residual and irradiated malignant glioma, with comparably reduced cellularity and mitotic activity, and near absent necrosis and endothelial hyperplasia. The irradiated tumor retained the perivascular formations and pseudorosettes, cellular elongation, and EMA dot-like immunostaining. In addition, subpial palisading was seen on this post-irradiation specimen. Again, these morphological features were consistent with high-grade glioma. For this post-radiation recurrence, the patient was treated with dose-intense temozolomide as per the ACNS-0126 protocol. His subsequent MR imaging has remained stable without evidence of recurrence to date. He has experienced some worsening and improvement of neurologic symptoms since his second operation. In particular he complained of problems with balance and gait, expressive aphasia, and lower limb and left facial weakness. However, these symptoms improved with an adjustment of his medications (dexamethasone) and no further surgeries have been required to date.

Neuroradiology: Imaging characteristics of an unusual, high-grade angiocentric glioma: A case report and review of the literature.

Aguilar et al.

DISCUSSION

In the past decade, improvements in histopathologic techniques have allowed a level of differentiation of central nervous system (CNS) tumor subtypes that was not previously achievable. Thus, CNS tumors have undergone re-classification according to the international classification of human tumors published by the World Health Organization (WHO) [1]. Specifically, angiocentric gliomas (AGs) have been reclassified as a neuroepithelial CNS tumor, of uncertain etiology and histogenesis. AGs are a rare, slow growing neoplasm occurring predominantly in the pediatric population and in young adults without a strong gender bias, and most commonly presents with intractable seizures [2, 3]. The incidence is rare, with only 47 cases, including the present case thus far reported [2, 4-20]. Interestingly, of the total number of cases, 38 cases were of patients less than 20 years old, with the age predilection ranging from 2 - 70 years of age with a mean age of 14.6 ± 15.2 years. Restricting the analysis to patients less than 20 years old for all cases, the mean age becomes 8.3 ± 4.8 years. The ratio of males to females with this diagnosis is approximately 1.35, with 27 males and 20 females reported. These tumors are typically found in the cortex or subcortical white matter of any cerebral lobe [1, 21]. The risk factors for developing such a lesion are unknown. Most cases have been treated with either a subtotal or gross total surgical resection, with or without adjuvant radiotherapy. The prognosis is reportedly good with successful resection. The principal histologic features are an angiocentric growth pattern of elongated tumor cells that stain positively for EMA, GFAP, S-100, and vimentin but not for neuronal antigens. They have similar pathological features to infiltrating astrocytomas and ependymomas [22], and their rarity complicates accurate diagnosis [17].

Information concerning the imaging features of these entities remains scarce and prevents accurate primary imaging diagnosis of these lesions. We acknowledge that imaging findings for a solitary CNS tumor, particularly in the pediatric population, might not grossly affect the initial strategy of surgical intervention (gross total vs. subtotal resection). However, imaging plays a major role in guiding the approach to resection, as well as prognostication. Therefore, here we describe the imaging features of this unusual case of high-grade AG supported by histopathology, and discuss the ramifications for primary diagnosis of CNS tumors in the pediatric population.

The typical description of an AG on MR imaging is that of a supratentorial, superficial, well delineated, non-enhancing, T2- and FLAIR-hyperintense, T1-hypointense lesion [6, 7, 10-16, 21]. Of these descriptors, the least consistent among reports is the intensity of the T1 imaging signal, which ranges from hypo- to hyperintense. The tumor in the present case demonstrated moderate grade enhancement, particularly intense around the scattered central areas of cavitary necrosis. The outer solid rind of the tumor, however, did not demonstrate significant enhancement. The degree of central enhancement suggested a higher-grade tumor, with disruption of the blood-brain barrier. The predominantly solid nature of the mass, without a significant cystic component, was not

supportive of entities such as ganglioglioma [23], pleomorphic xanthoastrocytoma [24] or dysembryoplastic neuroepithelial tumor [25].

DWI has been useful for preoperative grading of CNS tumors by providing an objective parameter for comparison in the form of the ADC. ADC values and their ratios to normal white matter have been used to differentiate between different types of CNS tumors [26-28], and combination with other quantitative parameters might improve pre-operative grading of tumors [29, 30]. Here we have shown that the solid portion of the tumor in this case demonstrated an intermediate to low ADC value, similar to normal brain, which is more typical for moderate to highly cellular tumors like anaplastic ependymomas [23] and medulloblastomas [23, 31], rather than a juvenile pilocytic astrocytoma [32].

Attempts have been made to differentiate between CNS neoplasms by MR spectroscopic analysis of regional metabolites [33-35], characteristics of which might also influence prognosis [36]. In this case, the very high choline content and elevated choline/NAA ratio suggested the presence of rapid tumor growth and necrotic tissue, characteristics of higher-grade malignancies, including primitive neuroectodermal tumors [37]. While non-specific, the presence of elevated lactate in this tumor could indicate accumulation within necrotic regions.

Overall, the combination of imaging features suggested a supratentorial intraaxial tumor with mixed features, in keeping with de-differentiation within a lower grade underlying neoplasm. In contrast to many of the reported cases of AGs, our case did not present with seizures. This might account for the relatively late presentation in our patient, who is older than many patients previously diagnosed with AG (Table 2). As a result, the longer duration might have allowed for the development of higher-grade components within what would otherwise typically be a very low-grade neoplasm. The acute presentation with neurologic impairment in our patient might be, in fact, related to relatively recent development of those high-grade components, and with resultant increased inflammation, edema, mass effect and compression of the adjacent corticospinal fiber tracts.

In this patient, we employed DTT as a means to aid in neurosurgical planning by mapping eloquent neuronal fiber tracts displaced or infiltrated by the tumor. Such an approach has been suggested to have good success in preserving essential tracts with surgical resection and might also influence decision-making pre-operatively [38-40]. By demonstrating posterior displacement of the corticospinal tract in the right frontal lobe, the neurosurgeon received prospective information concerning the optimal route for approaching the lesion (right anterolaterally), and for careful debulking the tumor along its posterior extent. The patient subsequently had near total recovery of motor strength and sensation on his left side, with only a mild persistent left pronator drift.

The above findings are in contrast to those of the several entities we considered on our differential diagnosis (please see Table 1). Specifically, we considered that this lesion might

Neuroradiology: Imaging characteristics of an unusual, high-grade angiocentric glioma: A case report and review of the literature.

Aguilar et al.

represent a ganglioglioma [23] which on CT are of variable density, enhance with contrast and are commonly associated with calcification. The MR findings of a ganglioglioma show small, well-circumscribed lesions without edema with T1 hypointensity, T2 hyperintensity, and strong contrast enhancement.

The CT findings of a pleomorphic xanthoastrocytoma [24] are normally cystic and solid masses, or simply solid masses, with minimal or no edema, also showing calcification and hemorrhage. On MR these lesions appear as cystic masses that may contain nodules, or again a predominantly solid mass, that exhibits T1 isointensity, T2 hyperintensity and strong contrast enhancement.

In contrast, dysembryoplastic neuroepithelial tumors [25], are hypodense, wedge shaped, lesions in the cortical/subcortical areas with scalloping of inner table and calcifications in about a third of cases as seen on CT. The MR findings show well-circumscribed lesions with multiple cysts or pseudocysts, T1 and FLAIR hypointensity, T2 hyperintensity, and weak contrast enhancement.

On CT, medulloblastomas [23, 31] are solid hyperdense masses usually found in fourth ventricle and which enhance with contrast. On MR, these are seen with T1 iso- to hypointense signals, and with variable T2 signal intensity. In addition, medulloblastomas exhibit increased signal on DWI, and low ADC signals, with variable contrast enhancement.

Anaplastic ependymomas, are supratentorial lesions [22, 23] that appear as heterogeneous and edematous parenchymal masses, with approximately half showing calcification, and which enhance variably with contrast. On MR, these are T1 isointense, variably intense on T2 since their signal intensity depends on the cellularity of the lesion. Further, anaplastic ependymomas exhibit an intermediate ADC (between medulloblastoma and pilocytic astrocytoma), and heterogenous contrast enhancement on MR.

Lastly on our differential, we considered a juvenile pilomyxoid/pilocytic astrocytoma [22, 32]. On CT, these lesions are mixed solid/cystic masses with variable edema, and with their solid portions enhancing with contrast. On MR, they are T1 hypo- or isointense, with hyperintense T2 and FLAIR signals. Their ADC signals are high, and they do not enhance with contrast. All of these features are different from our findings of the lesion presented in this report, which we have attributed to an angiocentric glioma with suggestive features on histopathology.

In summary, this case of an unusual high-grade angiocentric glioma is instructive from the perspective of imaging-based primary diagnosis of pediatric CNS tumors. When encountering a supratentorial tumor with mixed features suggesting the presence of both high-grade and low-grade tumor, de-differentiation of a normally low-grade tumor such as angiocentric glioma should be considered, in addition to high-grade malignancies such as medulloblastoma or anaplastic ependymomas.
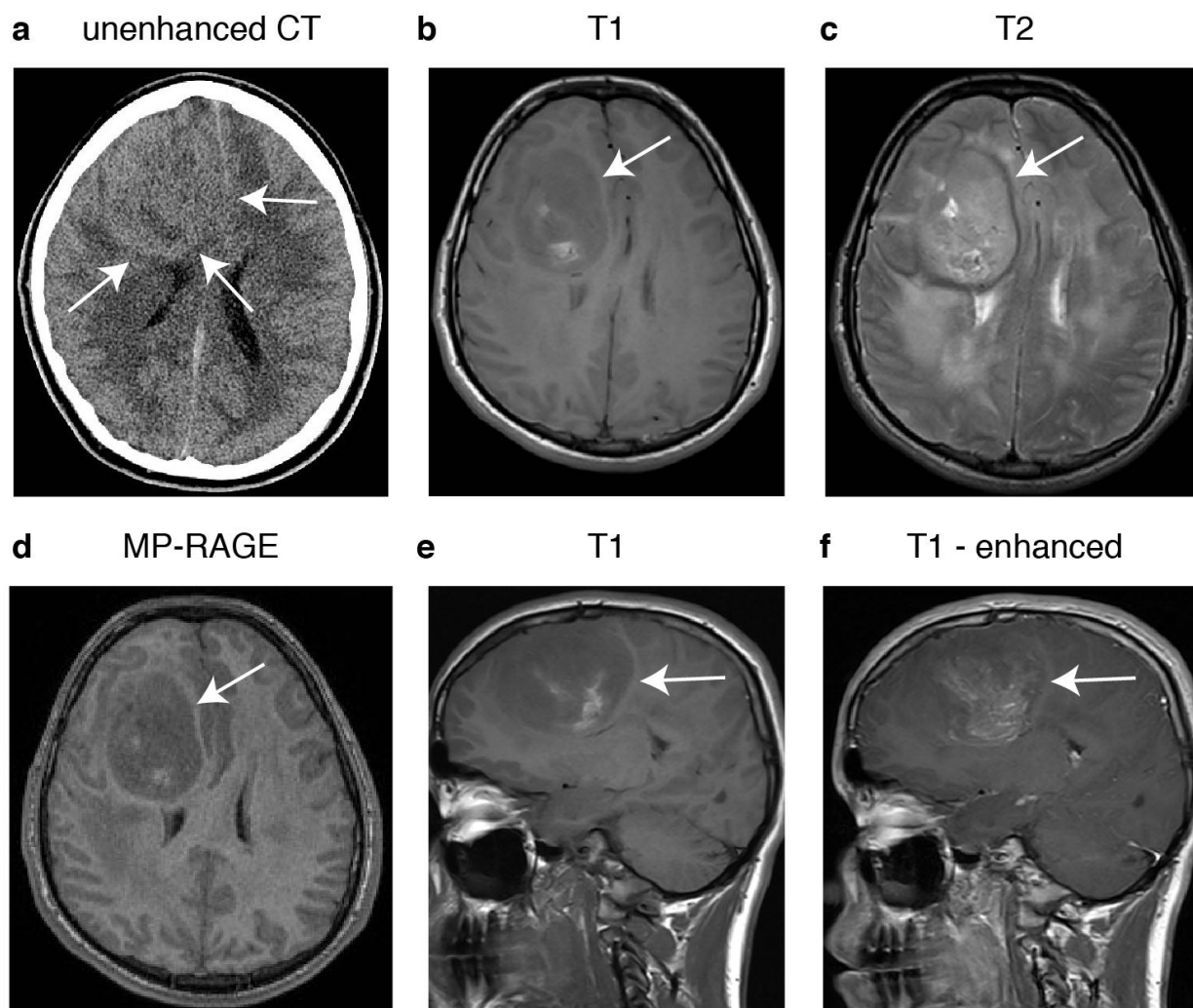
TEACHING POINT

When evaluating supratentorial tumors with mixed high- and low-grade features on magnetic resonance studies, consider the possibility of low-grade tumor de-differentiation, such as in an angiocentric glioma, in addition to high-grade malignancies such as medulloblastomas or anaplastic ependymomas.
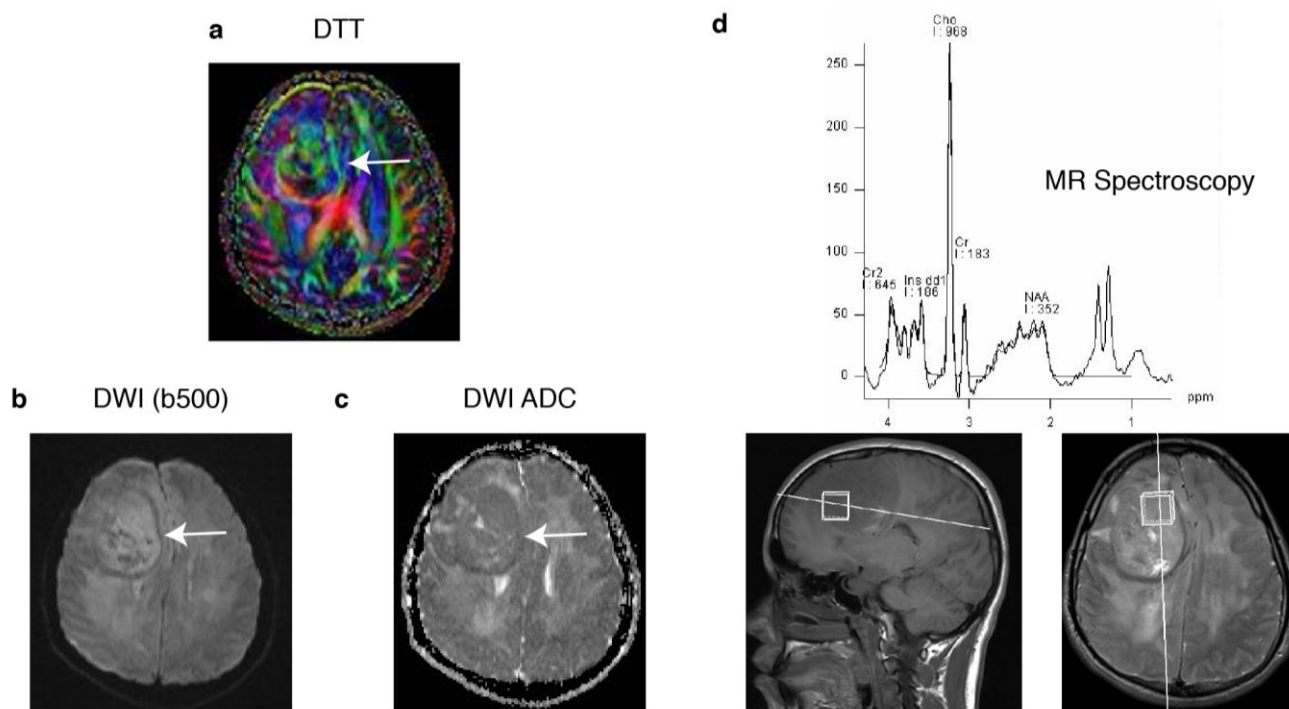
REFERENCES

1. Louis DN, Ohgaki H, Wiestler OD, et al. The 2007 WHO classification of tumours of the central nervous system. Acta Neuropathol. 2007;114:97-109. PMID: 17618441.
2. Marburger T, Prayson R. Angiocentric glioma: a clinicopathologic review of 5 tumors with identification of associated cortical dysplasia. Archives of pathology & laboratory medicine. 2011;135:1037-41. PMID: 21809996.
3. Prayson RA. Tumours arising in the setting of paediatric chronic epilepsy. Pathology. 2010;42:426-31. PMID: 20632818.
4. Fulton SP, Clarke DF, Wheless JW, Ellison DW, Ogg R, Boop FA. Angiocentric glioma-induced seizures in a 2-year-old child. J Child Neurol. 2009;24:852-6. PMID: 19304961.
5. Preusser M, Hoischen A, Novak K, et al. Angiocentric glioma: report of clinico-pathologic and genetic findings in 8 cases. Am J Surg Pathol. 2007;31:1709-18. PMID: 18059228.
6. Rosenzweig I, Bodi I, Selway RP, Crook WS, Moriarty J, Elwes RD. Paroxysmal ictal phonemes in a patient with angiocentric glioma. J Neuropsychiatry Clin Neurosci. 2010;22:123 E18-20. PMID: 20160231.
7. Ma X, Ge J, Wang L, et al. A 25-year-old woman with a mass in the hippocampus. Brain Pathol. 2010;20:503-6. PMID: 20438470.
8. Mott RT, Ellis TL, Geisinger KR. Angiocentric glioma: a case report and review of the literature. Diagn Cytopathol. 2010;38:452-6. PMID: 19941376.
9. Takada S, Iwasaki M, Suzuki H, Nakasato N, Kumabe T, Tominaga T. Angiocentric glioma and surrounding cortical dysplasia manifesting as intractable frontal lobe epilepsy--case report. Neurol Med Chir (Tokyo). 2011;51:522-6. PMID: 21785249.
10. Hu XW, Zhang YH, Wang JJ, Jiang XF, Liu JM, Yang PF. Angiocentric glioma with rich blood supply. J Clin Neurosci. 2010;17:917-8. PMID: 20399664.
11. Miyata H, Ryufuku M, Kubota Y, Ochiai T, Niimura K, Hori T. Adult-onset angiocentric glioma of epithelioid cell-predominant type of the mesial temporal lobe suggestive of a rare but distinct clinicopathological subset within a spectrum of angiocentric cortical ependymal tumors. Neuropathology. 2011. PMID: 22151480.
12. Li JY, Langford LA, Adesina A, Bodhireddy SR, Wang M, Fuller GN. The high mitotic count detected by phospho-histone H3 immunostain does not alter the benign behavior of angiocentric glioma. Brain Tumor Pathol. 2012;29:68-72. PMID: 21892765.
13. Koral K, Koral KM, Sklar F. Angiocentric glioma in a 4-year-old boy: imaging characteristics and review of the literature. Clin Imaging. 2012;36:61-4. PMID: 22226445.

14. Lellouch-Tubiana A, Boddaert N, Bourgeois M, et al. Angiocentric neuroepithelial tumor (ANET): a new epilepsy-related clinicopathological entity with distinctive MRI. Brain Pathol. 2005;15:281-6. PMID: 16389940.

15. Rho GJ, Kim H, Kim HI, Ju MJ. A case of angiocentric glioma with unusual clinical and radiological features. J Korean Neurosurg Soc. 2011;49:367-9. PMID: 21887397.

16. Shakur SF, McGirt MJ, Johnson MW, et al. Angiocentric glioma: a case series. J Neurosurg Pediatr. 2009;3:197-202. PMID: 19338465.

17. Lum DJ, Halliday W, Watson M, Smith A, Law A. Cortical ependymoma or monomorphous angiocentric glioma? Neuropathology. 2008;28:81-6. PMID: 18021197.

18. Sugita Y, Ono T, Ohshima K, et al. Brain surface spindle cell glioma in a patient with medically intractable partial epilepsy: a variant of monomorphous angiocentric glioma? Neuropathology. 2008;28:516-20. PMID: 18179412.

19. Wang M, Tihan T, Rojiani AM, et al. Monomorphous angiocentric glioma: a distinctive epileptogenic neoplasm with features of infiltrating astrocytoma and ependymoma. J Neuropathol Exp Neurol. 2005;64:875-81. PMID: 16215459.

20. Pokharel S, Parker JR, Parker JC, Jr., Coventry S, Stevenson CB, Moeller KK. Angiocentric glioma with high proliferative index: case report and review of the literature. Ann Clin Lab Sci. 2011;41:257-61. PMID: 22075509.

21. Amemiya S, Shibahara J, Aoki S, Takao H, Ohtomo K. Recently established entities of central nervous system tumors: review of radiological findings. J Comput Assist Tomogr. 2008;32:279-85. PMID: 18379318.

22. Lehman NL. Central nervous system tumors with ependymal features: a broadened spectrum of primarily ependymal differentiation? J Neuropathol Exp Neurol. 2008;67:177-88. PMID: 18344909.

23. Panigrahy A, Bluml S. Neuroimaging of pediatric brain tumors: from basic to advanced magnetic resonance imaging (MRI). J Child Neurol. 2009;24:1343-65. PMID: 19841424.

24. Crespo-Rodriguez AM, Smirniotopoulos JG, Rushing EJ. MR and CT imaging of 24 pleomorphic xanthoastrocytomas (PXA) and a review of the literature. Neuroradiology. 2007;49:307-15. PMID: 17205313.

25. Campos AR, Clusmann H, von Lehe M, et al. Simple and complex dysembryoplastic neuroepithelial tumors (DNT) variants: clinical profile, MRI, and histopathology. Neuroradiology. 2009;51:433-43. PMID: 19242688.

26. Murakami R, Hirai T, Kitajima M, et al. Magnetic resonance imaging of pilocytic astrocytomas: usefulness of the minimum apparent diffusion coefficient (ADC) value for differentiation from high-grade gliomas. Acta Radiol. 2008;49:462-7. PMID: 18415792.

27. Rumboldt Z, Camacho DL, Lake D, Welsh CT, Castillo M. Apparent diffusion coefficients for differentiation of cerebellar tumors in children. AJNR Am J Neuroradiol. 2006;27:1362-9. PMID: 16775298.

28. Yamasaki F, Kurisu K, Satoh K, et al. Apparent diffusion coefficient of human brain tumors at MR imaging. Radiology. 2005;235:985-91. PMID: 15833979.

29. Arvinda HR, Kesavadas C, Sarma PS, et al. Glioma grading: sensitivity, specificity, positive and negative predictive values of diffusion and perfusion imaging. J Neurooncol. 2009;94:87-96. PMID: 19229590.

30. Server A, Kulle B, Maehlen J, et al. Quantitative apparent diffusion coefficients in the characterization of brain tumors and associated peritumoral edema. Acta Radiol. 2009;50:682-9. PMID: 19449234.

31. Eran A, Ozturk A, Aygun N, Izbudak I. Medulloblastoma: atypical CT and MRI findings in children. Pediatr Radiol. 2010;40:1254-62. PMID: 20386894.

32. Lee IH, Kim JH, Suh YL, et al. Imaging characteristics of pilomyxoid astrocytomas in comparison with pilocytic astrocytomas. Eur J Radiol. 2011;79:311-6. PMID: 20619565.

33. Ishimaru H, Morikawa M, Iwanaga S, Kaminogo M, Ochi M, Hayashi K. Differentiation between high-grade glioma and metastatic brain tumor using single-voxel proton MR spectroscopy. Eur Radiol. 2001;11:1784-91. PMID: 11511902.

34. Server A, Josefsen R, Kulle B, et al. Proton magnetic resonance spectroscopy in the distinction of high-grade cerebral gliomas from single metastatic brain tumors. Acta Radiol. 2010;51:316-25. PMID: 20092374.

35. Wang Z, Sutton LN, Cnaan A, et al. Proton MR spectroscopy of pediatric cerebellar tumors. AJNR Am J Neuroradiol. 1995;16:1821-33. PMID: 8693982.

36. Girard N, Wang ZJ, Erbetta A, et al. Prognostic value of proton MR spectroscopy of cerebral hemisphere tumors in children. Neuroradiology. 1998;40:121-5. PMID: 9541923.

37. Panigrahy A, Krieger MD, Gonzalez-Gomez I, et al. Quantitative short echo time 1H-MR spectroscopy of untreated pediatric brain tumors: preoperative diagnosis and characterization. AJNR Am J Neuroradiol. 2006;27:560-72. PMID: 16551993.

38. Bagadia A, Purandare H, Misra BK, Gupta S. Application of magnetic resonance tractography in the perioperative planning of patients with eloquent region intra-axial brain lesions. J Clin Neurosci. 2011;18:633-9. PMID: 21371893.

39. Castellano A, Bello L, Michelozzi C, et al. Role of diffusion tensor magnetic resonance tractography in predicting the extent of resection in glioma surgery. Neuro Oncol. 2011. PMID: 22015596.

40. Yu CS, Li KC, Xuan Y, Ji XM, Qin W. Diffusion tensor tractography in patients with cerebral tumors: a helpful technique for neurosurgical planning and postoperative assessment. Eur J Radiol. 2005;56:197-204. PMID: 15916876.

www.RadiologyCases.com

Neuroradiology: Imaging characteristics of an unusual, high-grade angiocentric glioma: A case report and review of the literature.
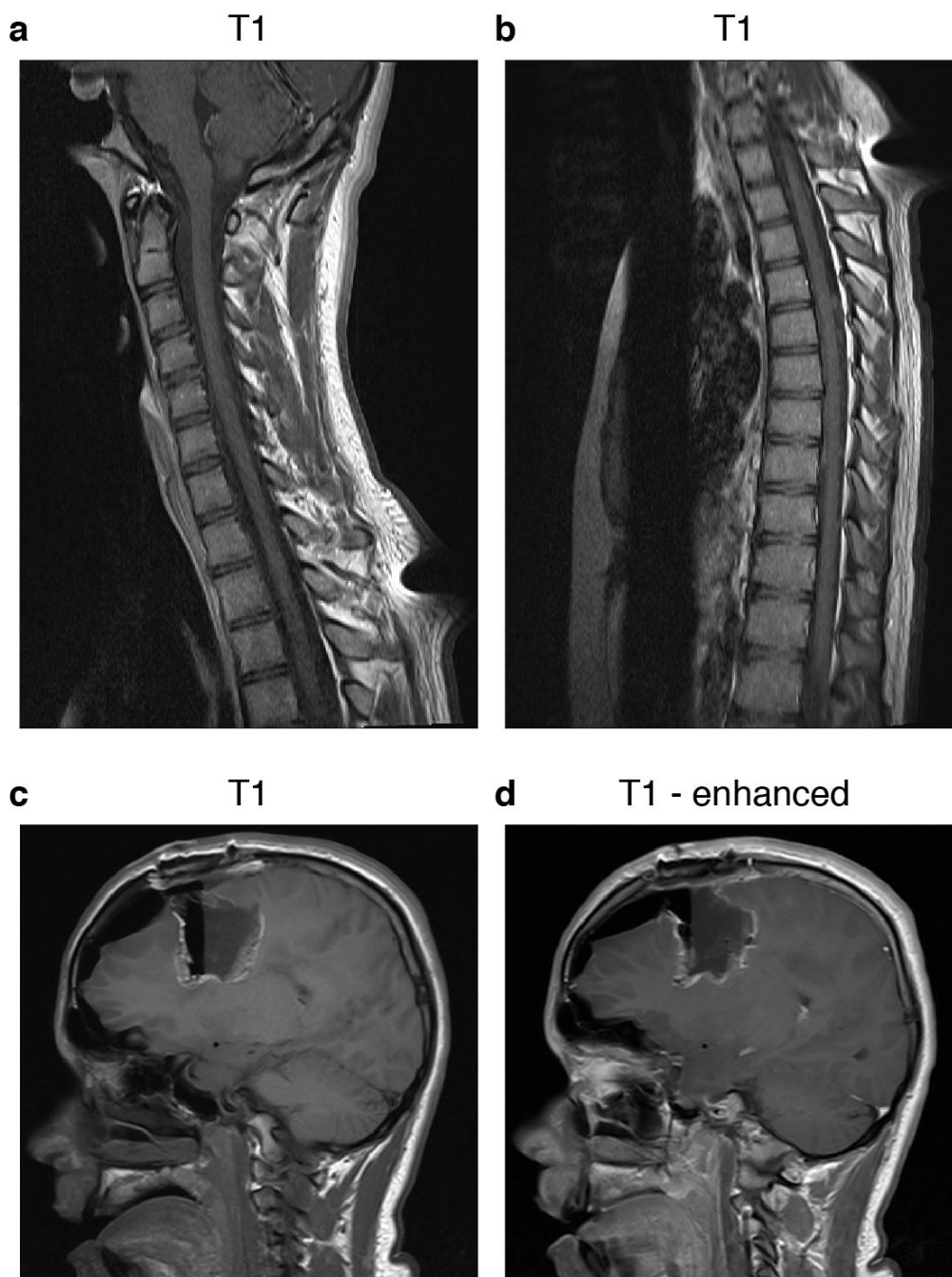
Aguilar et al.

FIGURES

Figure 1: CT and MR images of 15-year-old male with an angiocentric glioma in the right frontal lobe. a: Axial unenhanced CT image (Siemens SOMATOM Definition AS+, 64-slice multidetector CT, sequential axial, 287 mAs, 120 kVp, 4.8 mm slice thickness) demonstrating a heterogeneous mass centered on the right frontal lobe causing a mass effect and midline shift. b, c, d: Axial MR images from T1, T2 and magnetization-prepared rapid acquisition with gradient echo (MP-RAGE) studies corresponding to approximately the same plane as in panel a, and showing irregular areas of T1 hyperintensity within the central and inferior portions of the mass in keeping with hemorrhage. e and f: Sagittal T1 MR images without and with delayed gadolinium contrast enhancement (Gadovist, 0.2 ml/kg intravenously), demonstrating mild internal enhancement. Protocol: Siemens MAGNETOM Avanto 1.5T. T1: with TE of 12 msec, TR 283 msec, 5 mm slice thickness. MP-RAGE:3D gradient echo, TE 3.4 msec, TR 1900 msec. T2: TE 105 msec, TR 5662 msec, 5 mm slice thickness.

Neuroradiology: Imaging characteristics of an unusual, high-grade angiocentric glioma: A case report and review of the literature.

Aguilar et al.

Figure 2: MR images of 15-year-old male with an angiocentric glioma in the right frontal lobe. The axial images shown correspond to the same anatomic level. a: Axial diffusion tensor tractography (DTT) image. Red, blue, and green colors indicate diffusion of water molecules along the lateral, craniocaudal, and anteroposterior axes, respectively, showing fiber tract distortion around the right frontal mass. b: Axial diffusion weighted image (DWI, b value of 500) demonstrating low to intermediate signal within the lesion corresponding to intermediate cellularity. c: An axial DWI showing the apparent diffusion coefficient (ADC) map. d: MR spectroscopy of the frontal lobe lesion demonstrating signal peaks for choline (Cho), creatine (Cr), inositol (Ins), and N-acetyl aspartate (NAA) are shown (TE = 270 msec). The elevated choline peak is indicative of a high-grade lesion with rapid membrane turnover. A lactate doublet, confirmed by inversion of the peak at intermediate TE (not shown), is also suggestive of a higher-grade lesion with relative hypoxia. The white boxes in the sagittal T1 and axial T2 images below the graph demarcate the sampling volume used to obtain the spectra. Protocol: Siemens MAGNETOM Avanto 1.5T. DWI: TE 121 msec, TR 5200 msec, 5 mm slice thickness, with b factors of 0, 500 and 1000. DTT: TE 88 msec, TR 3236 msec, 5 mm slice thickness. MR spectroscopy was performed by selecting a 2.0 x 2.0 x 2.0 cm cube within a solid portion of the tumor anteromedially, and performing short (TE 30 msec), medium (TE 135 msec) and long (TE 270 msec) spectral acquisitions in this tissue volume.

Neuroradiology: Imaging characteristics of an unusual, high-grade angiocentric glioma: A case report and review of the literature.

Aguilar et al.

Figure 3: MR images of 15-year-old male with an angiocentric glioma in the right frontal lobe. a and b: Sagittal T1 MR images demonstrating the absence of lesions in the cervical and thoracic spinal cord regions. The spinal cord signal was unremarkable, with no enhancing masses seen. c and d: Sagittal T1 MR images without and with contrast (gadolinium) obtained 1 day post-resection. The large right frontal intraaxial mass was excised via a right frontal craniotomy, resulting in decompression of the right frontal horn of the lateral ventricle and a reduction in leftward midline shift to 0.6 cm from the initial 1.2 cm. Protocol: Siemens MAGNETOM Avanto 1.5T, with sagittal sequences using T1-weighted (T1, with echo time (TE) of 12 msec, TR 283 msec, 5 mm slice thickness). Enhancement was achieved by gadolinium administration (Gadovist, 0.2 ml/kg intravenously), which was followed by a sagittal T1 sequence (TE 12 msec, TR 382 msec).

a   T1 - enhanced   **d**   T2
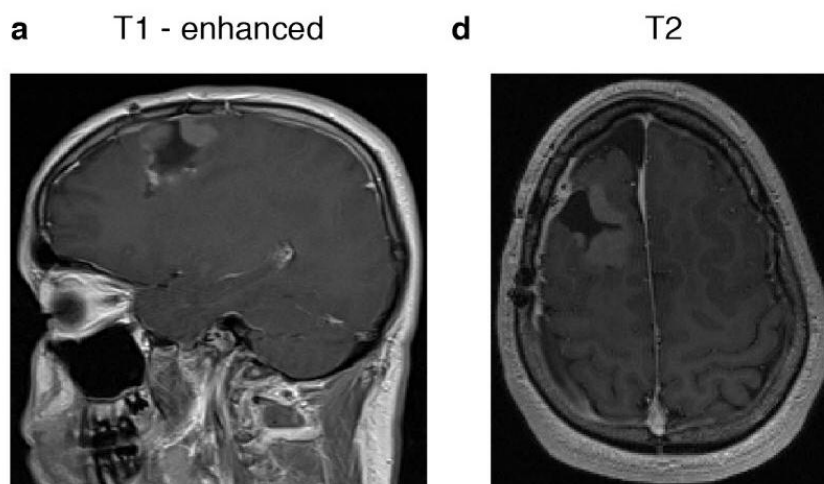
Figure 4: MR images of 15-year-old male with an angiocentric glioma in the right frontal lobe. a: Sagittal MR image from contrast-enhanced T1 sequence, demonstrating increased nodular thickened and enhancing tissue lining the resection cavity along its medial aspects measuring up to 1.4 cm in maximal thickness. In addition, there is slightly thickened and enhancing dura in the region of previous surgical resection. B: Axial T2 MR image demonstrating diffuse T2 hyperintense signal throughout the white matter of the cerebral hemispheres likely due to post-radiation changes. A subdural hygroma over the right cerebral hemisphere is also seen. Protocol: Siemens MAGNETOM Avanto 1.5T. T1: with TE of 12 msec, TR 283 msec, 5 mm slice thickness. MP-RAGE:3D gradient echo, TE 3.4 msec, TR 1900 msec. T2: TE 105 msec, TR 5662 msec, 5 mm slice thickness. Gadolinium contrast enhancement achieved with Gadovist, 0.2 ml/kg intravenously.

Entity	CT Findings	MR imaging Findings
Angiocentric Glioma [6, 7, 10-16, 21]	• Non-enhancing, ill-defined intraaxial mass	• T1: variable intensity signal • T2/FLAIR: hyperintense signal • Non-enhancing, or weak and irregular internal enhancement with contrast
Ganglioglioma [23]	• Variable density • Calcification common • About half enhance	• Small, well-circumscribed lesion without edema • T1: hypointense signal • T2: hyperintense signal • Strong contrast enhancement
Pleomorphic Xanthoastrocytoma [24]	• Cystic/solid mass, or just solid mass • Minimal or no edema • Calcification and hemorrhage	• Cystic mass that may contain nodules, or predominantly solid mass • T1: isointense signal • T2: hyperintense signal • Strong contrast enhancement
Dysembryoplastic Neuroepithelial Tumor [25]	• Hypodense • Wedge shaped, cortical/subcortical, with scalloping of inner table • Calcifications in about a third of cases	• Well-circumscribed, multiple cysts or pseudocysts • T1: hypointense signal • T2: hyperintense signal • FLAIR: hypointense • Weak contrast enhancement
Medulloblastoma [23, 31]	• Solid hyperdense mass in 4th ventricle • Enhances with contrast	• T1: iso- to hypointense signal • T2: variable intensity signal • DWI: increased signal • ADC: low signal • Variable enhancement with contrast
Anaplastic Ependymoma, supratentorial [22, 23]	• Heterogeneous parenchymal mass • Half exhibit calcification • Surrounding edema • Variable enhancement	• T1: isointense signal • T2: variable intensity signal depending on cellularity • Intermediate ADC (between medulloblastoma and pilocytic astrocytoma) • Heterogeneous contrast enhancement
Juvenile Pilomyxoid/Pilocytic Astrocytoma [22, 32]	• Mixed solid/cystic mass • Variable edema • Solid portion enhances with contrast	• T1: hypo- or isointense signal • T2/FLAIR: hyperintense signal • ADC: high signal • No contrast enhancement

Table 1: Differential diagnosis table for angiocentric glioma

Neuroradiology: Imaging characteristics of an unusual, high-grade angiocentric glioma: A case report and review of the literature.

Aguilar et al.

Etiology:	Categorized as a neuroepithelial tumor, but true histogenesis remains unknown.
Incidence:	Rare; 47 cases, including the present case, have been reported. Of those, 38 cases were of patients less than 20 years old. [2, 4-20]
Gender ratio:	Of the 47 cases, 27 males and 20 females are reported (ratio of M to F: 1.35).
Age predilection:	Range: 2 – 70 years, mean age of 14.6 ± 15.2 years. Restricting the analysis to patients less than 20 years old, the mean age becomes 8.3 ± 4.8 years.
Risk factors:	Unknown.
Treatment:	Subtotal or gross total surgical resection, with or without adjuvant radiotherapy.
Prognosis:	Reportedly good with successful resection.
Findings on imaging:	MR: supratentorial, superficial, well delineated, non-enhancing, T2- and FLAIR-hyperintense, T1-hypointense lesion [6, 7, 10-16, 21].

Table 2: Summary table for angiocentric glioma

ABBREVIATIONS

ADC = apparent diffusion coefficient
AG = angiocentric glioma
Cho- choline
cm = centimeter
CNS = central nervous system
Cr = creatine
CT = computed tomography
DTT = diffusion tensor tractography
DWI = diffusion weighted imaging
EMA = epithelial-membrane antigen
FLAIR = fluid attenuated inversion recovery
GFAP = Glial fibrillary acidic protein
Gy = gray
Ins = inositol
mm = millimeter
MP-RAGE = magnetization-prepared rapid acquisition with gradient echo
MR = magnetic resonance
msec = milliseconds
NAA = N-acetyl aspartate
s = seconds
T = tesla
T1 = T1-weighted (MR imaging)
T2 = T2-weighted (MR imaging)
TE = echo time
WHO = World Health Organization

KEYWORDS

angiocentric glioma; MR imaging; MR tractography; diffusion tensor imaging; MR spectroscopy

Online access

This publication is online available at:
www.radiologycases.com/index.php/radiologycases/article/view/1134

Peer discussion

Discuss this manuscript in our protected discussion forum at:
www.radiolopolis.com/forums/JRCR

Interactivity

This publication is available as an interactive article with scroll, window/level, magnify and more features.
Available online at www.RadiologyCases.com

Published by EduRad

www.EduRad.org